crystals

Article

Preparation and Properties of RDX@FOX-7 Composites by Microfluidic Technology

Jin Yu, Hanyu Jiang, Siyu Xu, Heng Li, Yiping Wang, Ergang Yao, Qing Pei, Meng Li, Yang Zhang and Fengqi Zhao *

Science and Technology on Combustion and Explosion Laboratory, Xi'an Modern Chemistry Research Institute, Xi'an 710065, China
* Correspondence: npecc@163.com

Abstract: 1,3,5-trinitro-1,3,5-triazacyclohexane (RDX) is a type of high energy explosive, its application in weapon systems is limited by its high mechanical sensitivity. At the same time, 1,1-diamino-2,2-dinitroethylene (FOX-7) is a famous insensitive explosive. The preparation of RDX@FOX-7 composites can meet the requirements, high energy and low sensitivity, of the weapon systems. It is difficult for the reactor to achieve uniform quality of composite material, which affects its application performance. Based on the principle of solvent-anti-solvent, the recrystallization process was precisely controlled by microfluidic technology. The RDX@FOX-7 composites with different mass ratios were prepared. At the mass ratio of 10%, the RDX@FOX-7 composites are ellipsoid of about 15 μm with uniform distribution and quality. The advantages of microscale fabrication of composite materials were verified. The results of structure characterization showed that there is no new bond formation in RDX@FOX-7, but the distribution of two components on the surface of the composite was uniform. Based on the structure characterization, we established the structure model of RDX@RDX-7 and speculated the formation process of the composites in microscale. With the increase of FOX-7 mass ratios, the melting temperature of RDX was advanced, the thermal decomposition peak of RDX changed to double peaks, and the activation energy of RDX@FOX-7 composite decreased. These changes were more pronounced between 3 and 10% but not between 10 and 30%. The ignition delay time of RDX@FOX-7 was shorter than that of RDX and FOX-7. RDX@FOX-7 burned more completely than RDX indicating that FOX-7 can assist heat transfer and improve the combustion efficiency of RDX.

Keywords: composite explosives; microfluidic; laser ignition; RDX@FOX-7; thermal analysis; micro-Raman

check for updates

Citation: Yu, J.; Jiang, H.; Xu, S.; Li, H.; Wang, Y.; Yao, E.; Pei, Q.; Li, M.; Zhang, Y.; Zhao, F. Preparation and Properties of RDX@FOX-7 Composites by Microfluidic Technology. *Crystals* **2023**, *13*, 167. https://doi.org/10.3390/cryst13020167

Academic Editors: Rui Liu, Yushi Wen, Weiqiang Pang and Robert F. Klie

Received: 15 December 2022
Revised: 11 January 2023
Accepted: 15 January 2023
Published: 18 January 2023

1. Introduction

With the development of modern weapon systems, ammunition requires not only higher energy levels and energy release efficiency [1] but also a higher security in the process of preparation, storage, transportation, and combat readiness [2]. Therefore, high energy insensitive explosives have become an important direction for modern ammunition development [3]. RDX is a type of high energy explosive with good stability, which is often used in propellant as a high energy additive. However, the high mechanical sensitivity limits its application in weapon system [4]. At present, the research on reducing the sensitivity of RDX, whether to improve the crystal quality or to cover the insensitive material, has been very thorough [4–8]. Shi [9] and Guo [10] prepared RDX-based composite energetic microspheres with narrow particle size distribution. The particle size changes from 50~200 μm to 0.5~7 μm, and dense coating by polymer coating, which improved the thermal safety and mechanical sensitivity of RDX.

Furthermore, it was expected that the energy properties of the explosives can be maintained or even improved while desensitizing treatment [11]. FOX-7 has stable molecular structure and excellent comprehensive properties, exists in α phase under normal temperature, and normal pressure [12–14]. Its crystal density is 1.878 g·cm^{-3}, detonation velocity is 8870 m·s^{-1}, detonation pressure is 34.0 GPa, detonation energy is high, and it is insensitive to impact, spark, and friction [15]. What matters is that it is compatible with RDX. Gao [16] and Wei [17] employed theoretical methods including molecular dynamics (MD) simulation and quantum-chemical DFT and MP2 calculation to estimate the properties of 2,4,6,8,10,12-hexanitrohexaazaisowurtzitane; 1,3,5,7-tetranitro-1,3,5,7-tetrazacyclooctane; and FOX-7 co-crystal, respectively. The result indicates that CL-20/FOX-7 co-crystal may have the high forming probability in a molar ratio of 1:1 and meet a given standard of low sensitive high energetic materials. There is no research on RDX@FOX-7 co-crystal. Tian [18] has prepared pressed explosives containing FOX-7 and RDX. It was found that FOX-7 can improve the rapid ignition growth of RDX. Zhou [19] used the principle of solvent–nonsolvent to cover FOX-7 on the surface of RDX. When the mass ratio of FOX-7 to RDX was 3:1, the impact sensitivity of RDX was reduced from 80 to 32%, achieving a positive impact on security performance. However, the distribution uniformity of RDX and FOX-7 is poor and unstable. This is due to that it is inevitable that there exists a large range of concentration gradient and temperature gradient in the reactor, which makes the reaction environment in different regions of the reactor vary greatly, resulting in different crystalline forms after recrystallization, polycrystalline particles and single crystal particles are often doped [20]. The material quality is not easy to control.

In recent years, microfluidic technology has gradually emerged in the field of synthesis and preparation of energetic materials. Microfluidic technology is to process or manipulate microfluids in micropipes [21], which can realize the rapid and uniform mixing of multifluids in microscale. It is widely used in the fields of fine chemicals preparation [22], nanofunctional materials preparation [23], and so on [24]. The recrystallization process can be controlled precisely in microscale [25], so it is suitable for preparing explosives with small particle size and narrow distribution. Wu [26] used this technique to obtain nano-RDX particles ranging from 150 to 900 nm. Based on these characteristics, microfluidic technology has unique advantages in the preparation of composite explosives. Zhou illustrated the key to the preparation of Pb·BaTNR co-crystal is to enable the Stephen acid group to be able to combine lead ions and ions at the same time, which can be achieved by providing limited ion concentration and reaction space through the microfluidic technology, but not in the reactor. Similarly, a series of composite explosives, such as HNS@NC [27], nAl@PVDF@CL-20 [28], combustion catalyst A@NC, Pb(N3)2@NC [29], Zr@NC [30], TATB/F2602 [31], and HMX/F2602 [23], were prepared by continuous phase extraction. All the components in these composite explosives are physically compound, and there is no new chemical bond to form. The quality of the composite explosive is controlled by concentration and flow rate [32,33]. Generally speaking, composite explosives have two forms of co-crystal and coating. Actually, there are many different combinations of components; however, no reports have explored this.

It is very valuable to realize the crystal quality treatment and coating desensitization in one step, through the integration of technology upgrades. In this paper, RDX@FOX-7 composite with uniform quality was prepared by microfluidic technology based on the solvent–nonsolvent method. The advantages of microfluidic control are demonstrated by the characterization of the morphology, structure, and uniformity of RDX@FOX -7, which is expected to provide new ideas for the preparation of high quality composite explosives. The thermal decomposition characteristics and laser ignition characteristics are also investigated to provide basic data for its application.

2. Experimental Details

2.1. Raw Materials

RDX was provided by Gansu Yinguang Chemical Industry Group Co.,Ltd. (Yinguang, China). FOX-7 was produced by Xi'an Modern Chemistry Research Institute. Dimethyl sulfoxide (DMSO) was purchased from Chengdu Cologne Chemical Co.,Ltd. (Chengdu, China). The deionized water was made in the laboratory.

2.2. Preparation of RDX@FOX-7 Composite

RDX was dissolved in DMSO with a concentration of 0.03 g/mol. FOX-7 was added in various mass percentages (3%, 10%, 30%) to the solution and stirred until completely dissolved as the solvent phase. Deionized water was selected as the non-solvent phase. The two-phase solution was injected into the microfluidic chip at the flow rates of 1 and 5 mL/min, respectively by the driving device. The samples were filtered out as suspension and washed several times with deionized water to remove the residual solvent, and RDX@FOX-7 composites were obtained by freeze drying method. The production flow chart is showed in Figure 1. The microreactor used in the microfluidic system is heart-shaped, with high mixing efficiency, and the depth is 700 μm. In order to avoid blocking, the pipe connected at the outlet has an inner diameter of 1 mm and a length of 0.3 m.

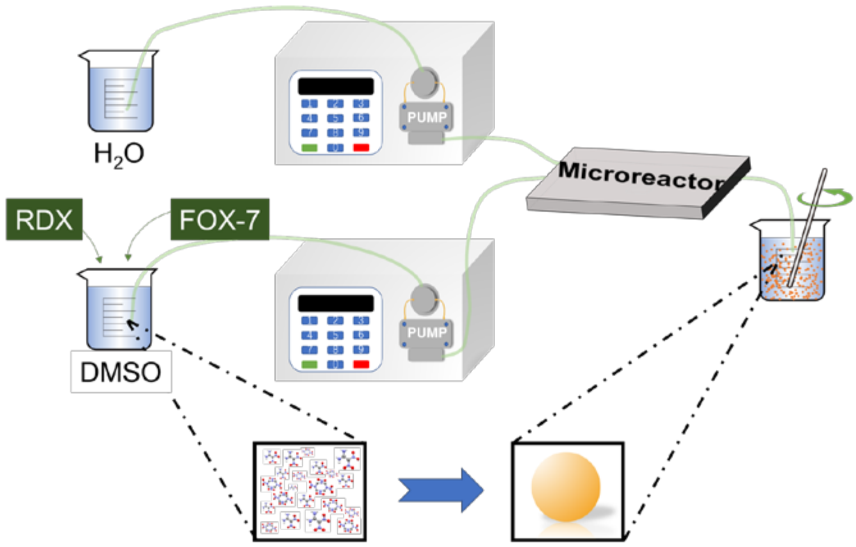

Figure 1. The flowchart for preparation of RDX@FOX-7 with microfluidic device.

2.3. Characterization Methods

The morphology of the sample was observed by scanning electron microscopy (SEM, FEI JSM-5800). The structure and composition were analyzed using X-ray diffraction (XRD, PANalytical Empyrean, Shanghai, China) and Fourier transform infrared spectroscopy (FT-IR, Tensor 27, Bruker, Germany). The quality of the composite was evaluated by a micro-Raman spectrometer (INVIAnvia type, spatial resolution is 1μm). In order to avoid the accumulation of thermal effects, it is necessary to test random sampling points, and the distance between two points should be greater than 1 mm. The effect of FOX-7 content on thermal decomposition characteristics of RDX was studied by differential scanning calorimeter (DSC, 200 F3, NETZSCH, Selb, Germany) with a heating rate of 5, 10, 15, 20 °C·min^{-1}, respectively (sample mass of (0.5 ± 0.2) mg, using an aluminum crucible with holes, normal pressure, and nitrogen flow rate of 50 mL/min). Kissinger, Ozawa, Friedman, and Starink methods were employed to obtain the activation energies of RDX@FOX-7 with different content (Equations (1)–(4)).

$$\ln\left(\frac{\beta}{T_p^2}\right) = \ln\left(\frac{AR}{E_k}\right) - \frac{E_k}{R}\frac{1}{T_p} \tag{1}$$

$$\lg\beta = \lg\left[\frac{AE_O}{RG(\alpha)}\right] - 2.315 - 0.4567\frac{E_O}{RT_p} \tag{2}$$

$$\ln\left(\beta\frac{d\alpha}{dT_p}\right) = \ln[Af(\alpha)] - \frac{E_F}{RT_p} \tag{3}$$

$$\ln\left(\frac{\beta}{{T_p}^{1.92}}\right) = \text{Const} - 1.0008\frac{E_S}{RT_p} \quad (4)$$

where E_k, E_O, E_F, and E_S are the activation energy with different content; T_p is thermal decomposition peak temperature; β is heating rate; R is universal gas constant; and A is pre-exponential factor.

3. Results and Discussion

3.1. Morphological and Structure Analysis

For explosives, morphological is very important for security performance. When stimulated by the outside, the irregular particles are easy to form hot spots at the corners. The spherical-like crystal has a smooth surface without edges and angles, less accumulation of hot spots, and mechanical sensitivity will be reduced. Smaller particle size also facilitates hot spot dispersion. Figure 2 shows electron microscopic images of RDX, FOX-7, and RDX@FOX-7. It is evident that the RDX crystal has the characteristics of smooth surface and large size. FOX-7 crystal is more irregular. The morphology and particle size distribution of RDX@FOX-7 are significantly different from those of the raw materials. When the mass ratio of FOX-7 is 3%, FOX-7 is adsorbed on the surface of the RDX particles in the form of small particles. This may be due to the low supersaturation of FOX-7 in the solution, which leads to the late crystallization point. When RDX reaches the equilibrium of dissolution and RDX crystal reaches the growth limit, FOX-7 begins to precipitate slowly, which results in the formation of such surface adsorption. When the FOX-7 mass ratio is 10%, it is much better, the particle size of RDX@FOX-7 was reduced obviously, about 15μm. On the other hand, RDX@FOX-7 is similar to RDX in shape of ellipsoid, and its surface is smooth without obvious edges and defects. RDX cannot be distinguished from FOX-7 by the SEM images, which indicates that the composite may be in the form of coating or co-crystal. When the mass ratio of FOX-7 was 30%, some larger particles appeared, which made the overall consistency of the composite worse. Therefore, it is concluded that 10% RDX@FOX-7 composite explosive has better comprehensive performance. Compared with the RDX@FOX-7 prepared in the reactor [19], which can be defined as the bonding of two component particles, the microfluidic technique has obvious advantages in morphology control.

Eutectic is a type of multi-component molecular crystal which is formed in the same lattice by non-covalent bond. When co-crystal is formed, the crystal structure and internal composition of each component changes radically. If the result is RDX@FOX-7 co-crystal, there must be a new bond formation. Thus, the composite was further characterized by XRD and FT-IR, and the results are showed in Figures 3 and 4. Peaks at 13.3°, 18.1°, 22.2° and 15.2°, 28.2° were used as markers for RDX and FOX-7, respectively. Many characteristic peaks of RDX can be observed in RDX@FOX-7 with different mass ratios, and the peaks are stronger. This is because the main component of the composite is RDX. In the spectra of RDX@FOX-7 with mass ratios of 3%, there were no FOX-7 characteristic peaks at 15.2° and 28.2°. The two peaks became stronger with the increase of mass ratio of FOX-7. The formation of RDX@FOX-7 composite can be determined. However, despite the relative intensity of the diffraction peak has changed, there is no new diffraction peak shows that the RDX@FOX-7 composite explosive does not form co-crystal. In the infrared spectrum, we can observe that the amino absorption peaks of RDX@FOX-7 at 3423, 3332, 3298 cm^{-1} have a blue shift of 2~3 cm^{-1} wave number compared to FOX-7, the C-H bond stretching vibration peak at 3074 and 3000 cm^{-1} has a red shift of 2~3 cm^{-1} wave number compared to RDX, and the nitro adsorption peak at 1594 cm^{-1} has shifted compared to FOX-7 and RDX. This may be because the amino of FOX-7 and the nitro of RDX formed a part of the hydrogen bond after forming the composition. The interaction between the molecules is weak, which can only lead to a certain degree of amino, nitro absorption peak shift, but in the infrared spectrum of the generation of new absorption peak. Therefore, we infer that the prepared sample is a type of composite explosive.

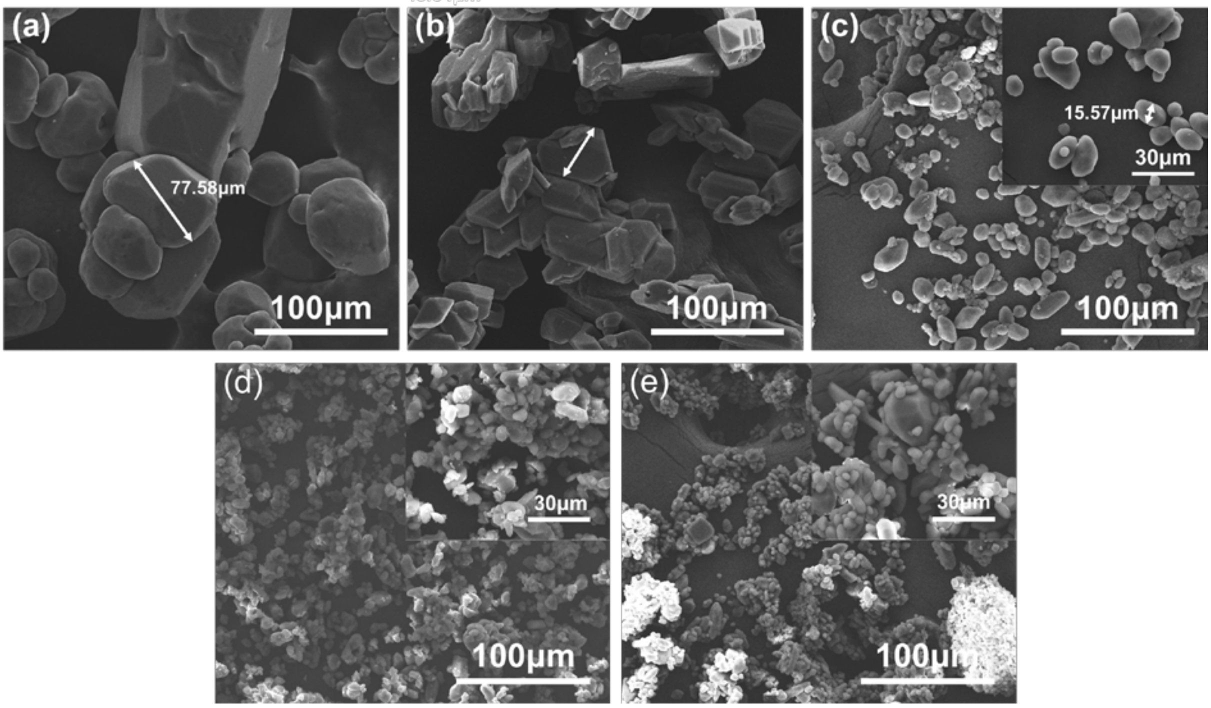

Figure 2. SEM images of samples: (**a**) raw RDX; (**b**) raw FOX-7; (**c**–**e**) RDX@FOX-7 with mass ratios of 10%, 3%, 30%.

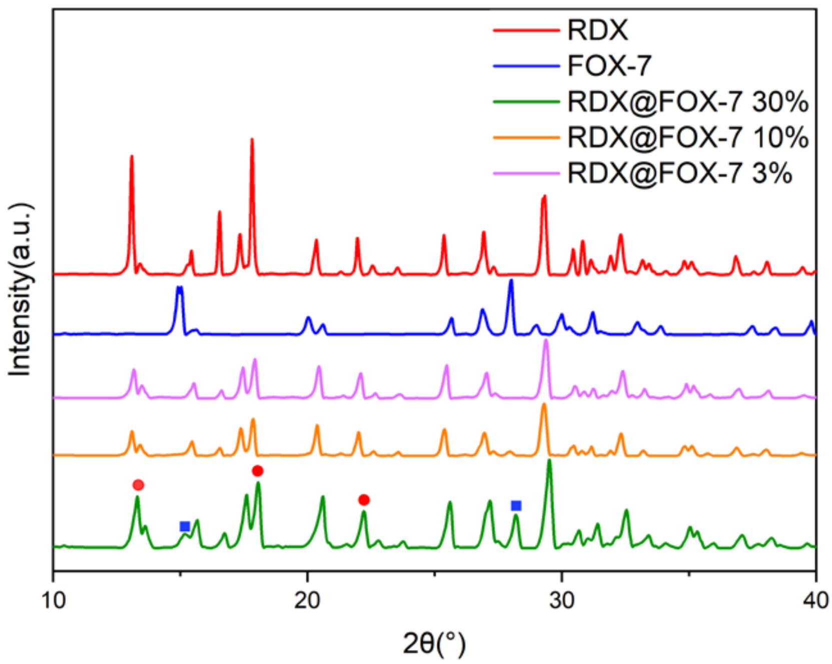

Figure 3. XRD patterns of the RDX, FOX-7, and RDX@FOX-7 composite.

Most composites have problems with uneven distribution These unevenly distributed composites are easy to be separated in use and cannot guarantee stable performance, which has a great impact on the reliability and service life of products. Raman spectroscopy can be used to identify the components distribution of composite by observing the characteristic peak of Raman characteristic peak. The crystal quality of RDX@FOX-7 was characterized by micro-Raman spectra at 10 different points, and the results are shown in Figure 5. It can be seen that the peak shape in the Raman spectra of each point has a good consistency. Seven important Raman peaks were observed. The characteristic peaks at 476 cm^{-1}, 1340 cm^{-1}, and 1548 cm^{-1} belong to the symmetric rocking vibration peak corresponding to N-H, the symmetric stretching vibration peak corresponding to C-NO_2, and the torsional vibration peak corresponding to NH_2 in FOX-7. Similarly, the characteristic peaks at 467 cm^{-1}, 923 cm^{-1}, 1274 cm^{-1}, 1311 cm^{-1}, 1388 cm^{-1}, and 1377 cm^{-1} belong to the tensile vibration of N-N, the rocking vibration of CH_2, the tensile vibration of N-NO_2 and the bending vibration outside the C-H plane in RDX, indicating that a type of composite explosive with excellent uniformity was achieved.

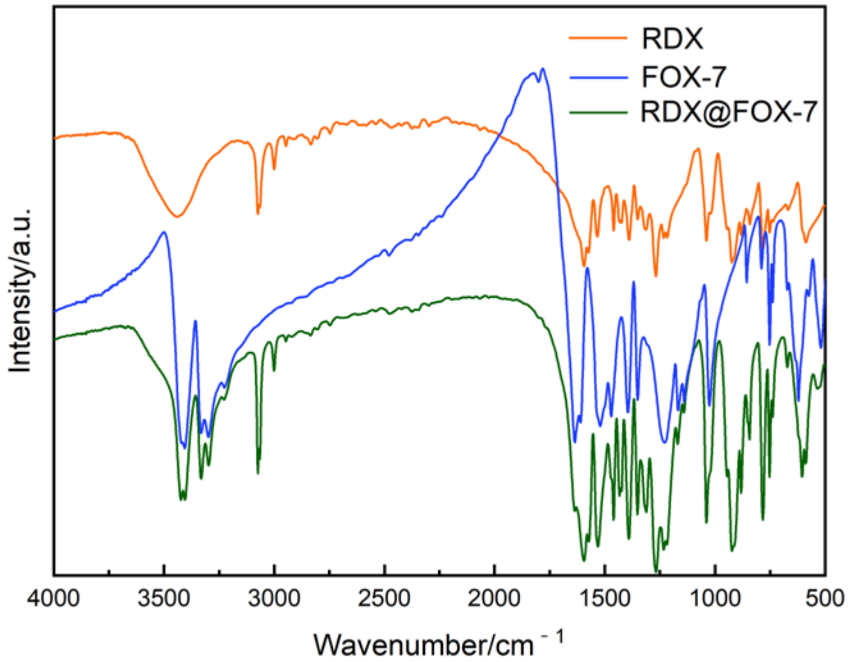

Figure 4. FT-IR spectra of the RDX, FOX-7, and RDX@FOX-7 composite with mass ratios of 10%.

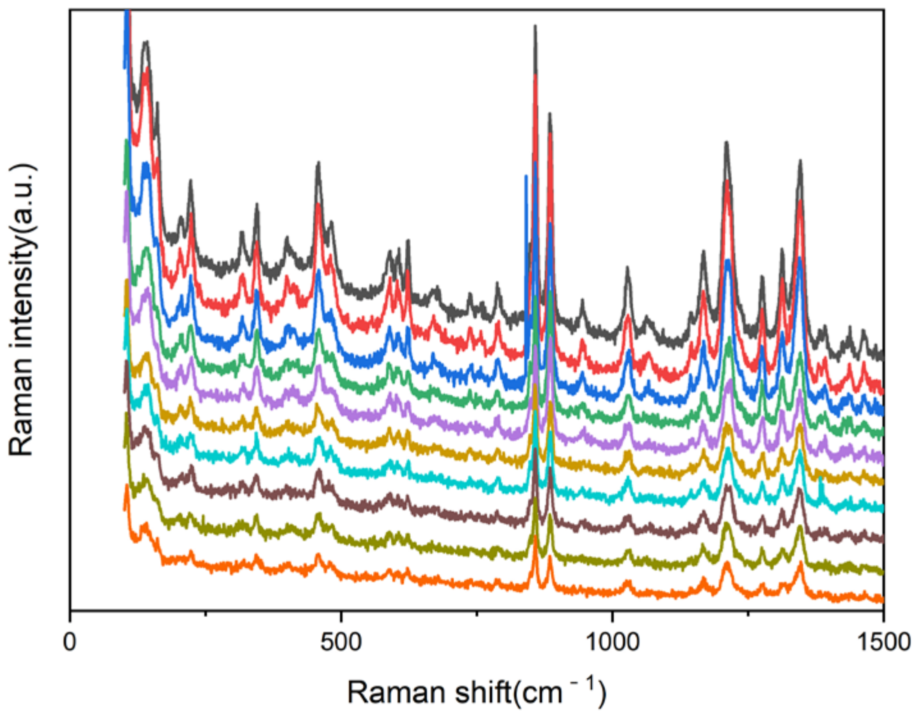

Figure 5. Micro-Raman spectra of RDX@FOX-7 at 10 different points.

Deeply, we modeled the structure of RDX@FOX-7 (shown in Figure 6). The reason for this effect lies in the formation of supersaturation, when two-phase solutions meet at the microscale, which causes the burst nucleation of crystals in a short time. Fluid mixing depends mainly on the diffusion of fluid molecules. The typical feature of microscale flow is that the Reynolds number (Re) is very low and the flow is mostly in the laminar flow region. It is very difficult to achieve efficient mixing without an external physical field. Therefore, we introduce disturbances through the structure of the microreactor to disrupt the stratified flow and enhance the mixing between the layers. Thus, the supersaturation of each point in the channel remains highly consistent and provides a stable driving force for crystal precipitation. In the pipe connected at the outlet, flow will maintain a uniform supersaturation, crystals continue to grow precipitation. Finally, the composite material with uniform distribution of two components is formed. Based on this, we believe that the uniformity of the composite material can be controlled by controlling the crystallization points of different components. When the crystallization points of two components are close, the uniform composite material such as RDX@FOX-7 is formed. When the process of two sets of crystals is independent in time, the composite material of the core shell structure can be obtained. Of course, we can also prepare more composite materials through other parameters, such as regulatory concentration and temperature, to meet the needs. It is interesting to be able to precisely control the internal structure of composites.

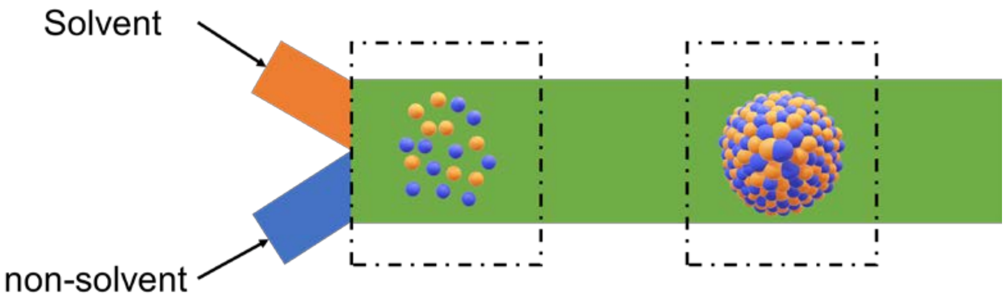

Figure 6. Structure model for RDX@FOX-7.

3.2. Thermal Behavior of RDX@FOX-7 Composite

Thermal decomposition is the initial stage of explosive combustion. The thermal decomposition characteristics of each component of composite explosive directly affect the combustion performance. The thermal decomposition properties of RDX@FOX-7 at different mass ratios were carried out by differential scanning calorimetry, as showed in Figure 7. The peak temperatures of thermal decomposition at various heating rates are listed in Table 1. Combined with DSC curve, the endothermic peak of $\alpha \rightarrow \beta$ and $\beta \rightarrow \gamma$ phase transition cannot be observed at about 116 °C and 145 °C when the content of FOX-7 is 3% and 10%. Thermal decomposition is the initial stage of explosive combustion. The thermal decomposition characteristics of each component of composite explosive directly affect the combustion performance. It can be seen that the melting endothermic peak of RDX is advanced with the increase of FOX-7 content, but the change is obvious between 3% and 10% of FOX-7 content, and it is advanced at about 4 °C. The effect of FOX-7 on the melting peak is not obvious, but the peak width and peak area increases, the heat needed for melting increases, and the thermal stability is better. At 10% of FOX-7, a sharp exothermic peak appears around 205 °C. This represents the first thermal decomposition of the FOX-7 with $\gamma \rightarrow \delta$ phase transition. In addition, with the increase of the heating rate, the peak temperature both of RDX@FOX-7 at different mass ratios moves to high temperature, the peak width becomes wider, the peak area increases, the heat release increases, and the reaction process becomes more complete. At the same heating rate, based on the two-step decomposition principle of FOX-7, with the content of FOX-7 increasing gradually, the heat release of the second decomposition increased, and the thermal decomposition of RDX gradually separated; the thermal decomposition peak of RDX@FOX-7 has a tendency to change from single peak to double peak.

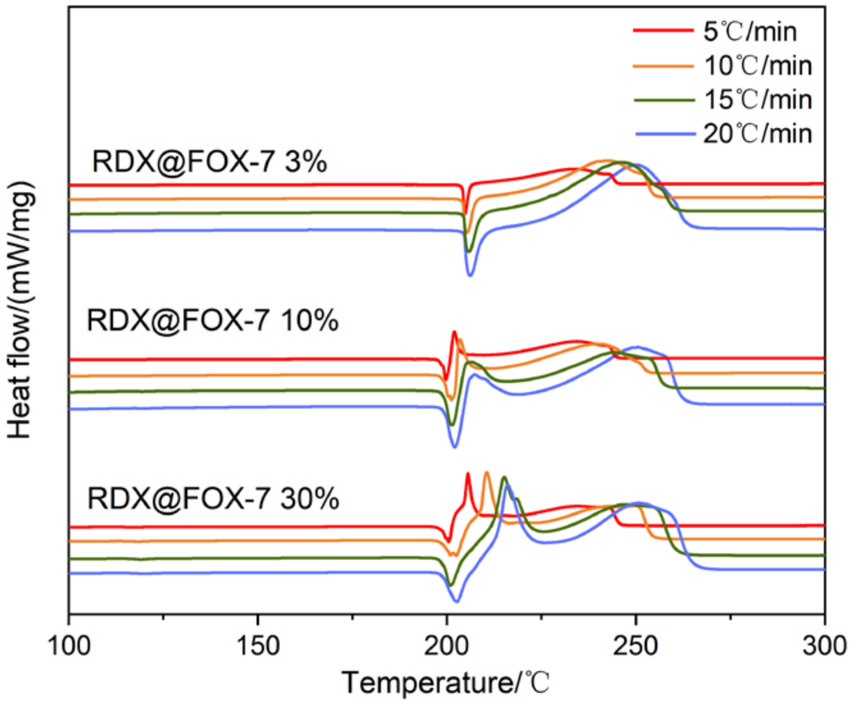

Figure 7. DSC curves of RDX@FOX-7 composite with different mass ratios at different heating rates.

Table 1. Thermal decomposition temperatures and kinetic parameters of RDX@FOX-7 with different mass ratios at different heating rates.

Sample	T_p/°C				E_O kJ/mol	E_K kJ/mol	E_F kJ/mol	E_S kJ/mol
	5 °C/min	10 °C/min	15 °C/min	20 °C/min				
RDX@FOX-7 3%	233.7	242.8	245.7	250.1	180.43	181.19	186.51	181.38
RDX@FOX-7 10%	234.2	239.7	244.3	250.5	178.36	179.00	185.40	179.19
RDX@FOX-7 30%	230.8	240.1	248.4	251.7	132.37	134.01	138.20	132.61

The thermal decomposition activation energy of RDX@FOX-7 samples were evaluated by the method of Kissinger, Flynn-Wall-Ozawa, Friedman, and Starink methods by using DSC data, and the results are showed in Table 1. The activation energy decreased with the increase of FOX-7 content from 3 to 10 %, which had little effect on the activation energy, about 1 KJ/mol. From 10 to 30 %, the activation energy decreased more obviously, about 40 KJ/mol. Combined with DSC data and activation energy calculation results, it can be fully demonstrated that FOX-7 has an obvious effect on improving the thermal stability of RDX. The effect of 10% addition of FOX-7 to RDX on the thermal stability was the best.

3.3. Ignition and Combustion Properties of RDX@FOX-7 Composite

Ignition is the beginning of combustion process, followed by pyrolysis reaction. Studying the ignition characteristics of RDX@FOX-7 can provide information support for its further application in the solid propellants. The ignition and combustion process of all samples were studied by using a laser ignition apparatus, which is shown in Figure 8. The radiation wavelength of the laser is 10.6 μm and the irradiation time is 5 ms. The time between the laser emission and the appearance of the flame is defined as the ignition delay time. The kinetics and mechanism of thermal decomposition affect the ignition delay time and flame structure, respectively. The change of ignition delay time with laser power density is shown in Figure 9. With the increase of laser power density, the ignition delay time first decreases rapidly and then tends to be constant. RDX@FOX-7 has a lower latency compared to RDX and FOX-7. This can be explained in relation to the results of thermal decomposition. The first thermal decomposition of the FOX-7 interacted with RDX, bringing the overall advance.

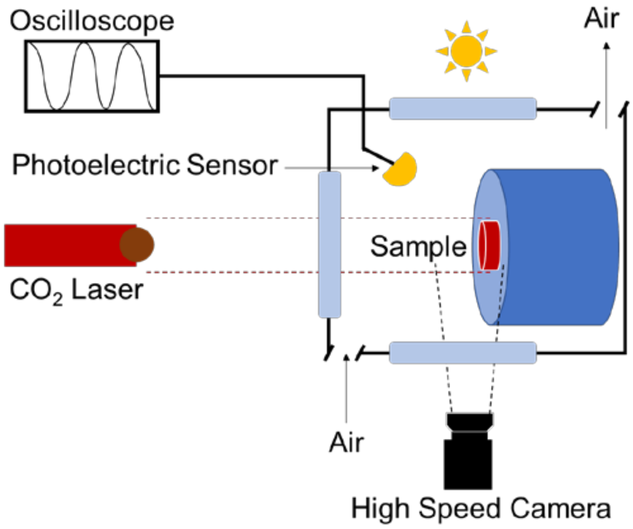

Figure 8. Schematic illustration of laser ignition apparatus.

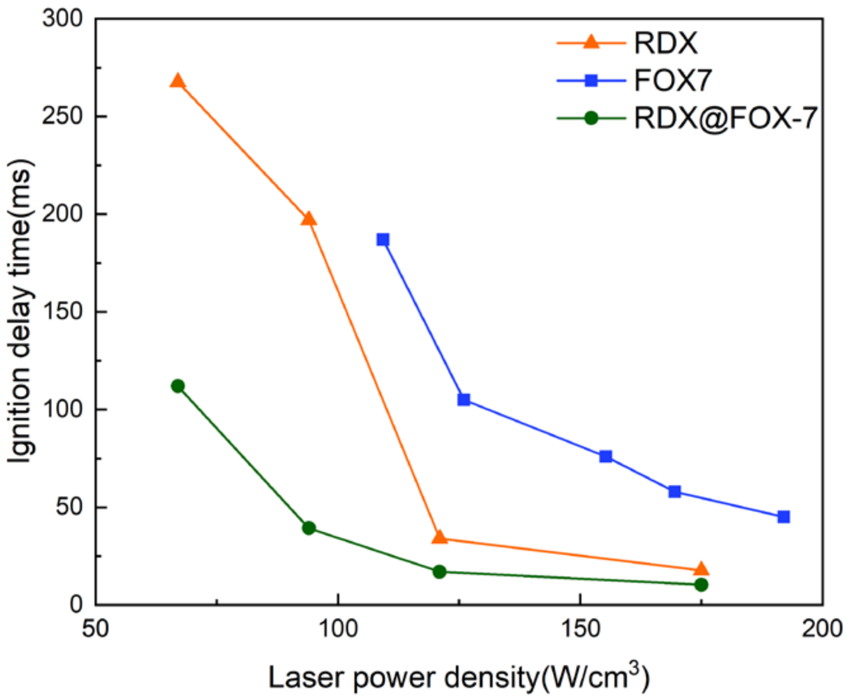

Figure 9. Ignition delay time of RDX, FOX-7 and RDX@FOX-7.

Figure 10 shows the combustion flame structures of RDX@FOX-7. When the laser power density is 169.5 W/cm^2, the ignited RDX powder has a dark red flame, and the inner layer is the bright core produced by the particle combustion. The further development of a more moderate flame has large gas clouds and more combustion of unreacted particles. It can be observed that there are melting surface and unreacted particles from the combustion residues of RDX shown in Figure 11a. Therefore, we infer that the accumulation of local heat due to the simultaneous melting and thermal decomposition of RDX will cause incomplete combustion. RDX@FOX-7 has a similar combustion flame evolution process. However, there are almost no unreacted particles, the complete combustion in the core of the flame lasts longer, the structure is stable, and the gas cloud area is smaller. Moreover, there are pores in the molten surface of the RDX@FOX-7 combustion residues, which is shown in Figure 11b, and the unreacted particles are obviously reduced. This may be due to the two thermal decompositions of FOX-7 experienced to spread the heat more evenly, accelerate the RDX melting heat of absorption, and, ultimately, make the combustion more complete. This is very critical for improving the application performance of RDX@FOX-7 in propellant. The unstable combustion of propellant is intermittent combustion, flameout during combustion, and incomplete chemical reaction. When the combustion of propellant is incomplete, it will destroy the internal ballistic performance of the engine and change the expected thrust plan. The addition of FOX-7 can ensure the energy output level to a certain extent, and it also has a high safety performance. In addition, as mentioned above, there is a very high application value for the auxiliary for RDX completely burning.

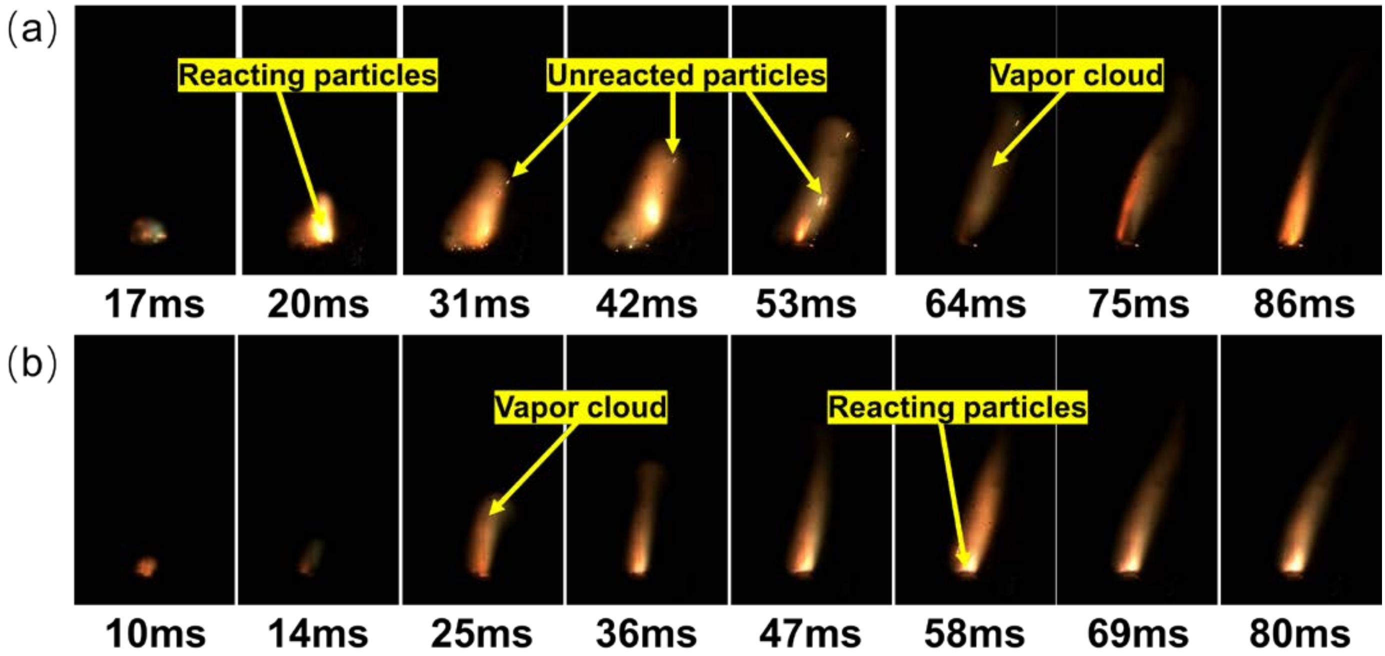

Figure 10. Sequential images for the combustion initial process of samples at the laser power density of 175 W/cm^2: (**a**) RDX, (**b**) RDX@FOX-7 composite.

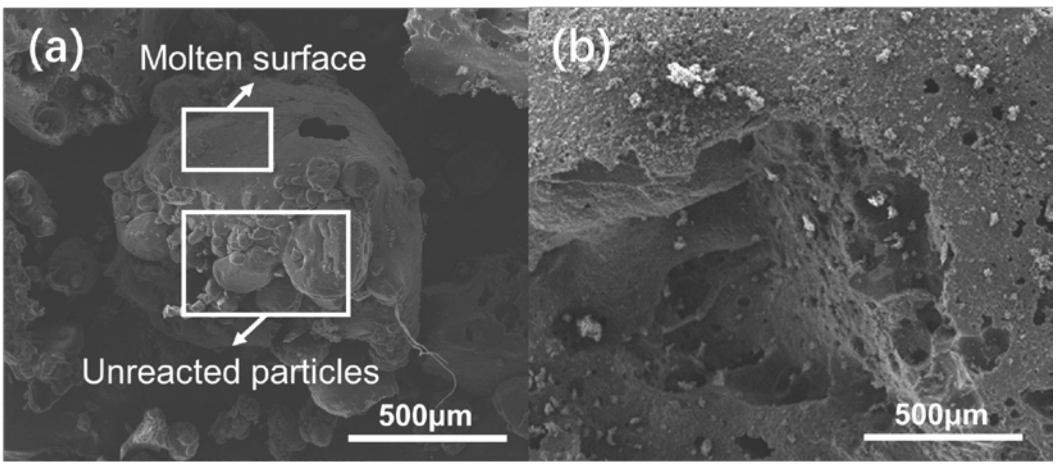

Figure 11. SEM images of the combustion residues of samples: (**a**) RDX, (**b**) RDX@FOX-7 composite.

4. Conclusions

(1) The RDX@FOX-7 composite with different mass ratios was successfully prepared by microfluidic technique. The structure was characterized by SEM, XRD, FT-IR, and micro-Raman. RDX@FOX-7 with 10% content has the best morphology, and the particle size is about 15 μm. The obtained composite explosive is of uniform distribution and uniform quality, and no co-crystal is formed.

(2) The advantages of microscale fabrication were verified. The structure model of RDX@FOX-7 is established. The formation process of the composites in microscale is predicted. It is considered that the uniformity of composites can be controlled by controlling the crystallization point of different components. In the future, more types of composites can be prepared by adjusting the concentration, temperature, and other parameters to meet the needs.

(3) With the increase of FOX-7 mass ratios, the melting temperature of RDX was advanced, the thermal decomposition peak of RDX changed to double peaks, and the activation energy of RDX@FOX-7 composite decreased. These changes were more pronounced between 3 and 10% but not between 10 and 30%.

(4) RDX@FOX-7 composite has a shorter ignition delay compared to RDX and FOX-7. FOX-7 can assist in heat transfer, making RDX@FOX-7 composite's combustion more complete.

In summary, the effect of a 10% addition of FOX-7 to RDX makes the overall comprehensive properties of the composites reach the best. This study provides a promising new method for the preparation of homogeneous and stable composites. Nevertheless, this study still has some limitations. For example, consider if the additional compressing tests would lead to specific reorientation of the crystals inside the composite, as well as a more comprehensive characterization of the applied properties of composite explosives. Next, we will also continue to study this in depth.

Author Contributions: S.X. and F.Z. contributed to the conception of the study; J.Y. and H.J. performed the experiments; Y.W., E.Y. and H.L. contributed significantly to analysis and manuscript preparation; J.Y. performed the data analysis and wrote the manuscript; Q.P., Y.Z. and M.L. helped perform the analysis with constructive discussions. All authors have read and agreed to the published version of the manuscript.

Funding: This work was financially supported by the National Natural Science Foundation of China (Funder: Jianhua Yi, Funding number: 22075226), (Funder: Yang Zhang, Funding number: 22205178).

Institutional Review Board Statement: Not applicable.

Informed Consent Statement: Informed consent was obtained from all subjects involved in the study.

Data Availability Statement: Not applicable.

Acknowledgments: The authors would like to gratefully thank Pang for his valuable suggestions to improve the quality of this article.

Conflicts of Interest: The authors declare no conflict of interest.

References

1. Jia, X.; Hou, C.; Wang, J.; Tan, Y.; Zhang, Y.; Li, C. Research Progress on the Desensitization Technology of Nitramine Explosives. *Chin. J. Explos. Propellants* **2018**, *41*, 326–333.
2. Liu, J.; Jiang, W.; Yang, Q.; Song, J.; Hao, G.-Z.; Li, F.-S. Study of nano-nitramine explosives: Preparation, sensitivity and application. *Def. Technol.* **2014**, *10*, 184–189. [CrossRef]
3. Sikder, A.; Sikder, N. A review of advanced high performance, insensitive and thermally stable energetic materials emerging for military and space applications. *J. Hazard. Mater.* **2004**, *112*, 1–15. [CrossRef] [PubMed]
4. Jia, X.; Hu, Y.; Xu, L.; Liu, X.; Ma, Y.; Fu, M.; Wang, J.; Xu, J. Preparation and Molecular Dynamics Simulation of RDX/MUF Nanocomposite Energetic Microspheres with Reduced Sensitivity. *Processes* **2019**, *7*, 692. [CrossRef]
5. Xu, W.; Deng, J.; Liang, X.; Wang, J.; Li, H.; Guo, F.; Li, Y.; Yan, T.; Wang, J. Comparison of the effects of several binders on the combination properties of cyclotrimethylene trinitramine (RDX). *Sci. Technol. Energ. Mater.* **2021**, *82*, 29–37.
6. Jia, X.; Cao, Q.; Guo, W.; Li, C.; Shen, J.; Geng, X.; Wang, J.; Hou, C. Synthesis, thermolysis, and solid spherical of RDX/PMMA energetic composite materials. *J. Mater. Sci. Mater. Electron.* **2019**, *30*, 20166–20173. [CrossRef]

7. Li, N.; Xiao, L.; Jian, X.; Xu, F.; Zhou, W. Coating of RDX with GAP-based energetic polyurethane elastomer. *J. Solid Rocket Technol.* **2012**, *35*, 212–215.
8. Zhang, J.; Zhang, J.; Wang, B.; Liu, S.; Zhang, T.; Zhou, D. Technology of Ultra-fine RDX Coating with Rapid Expansion of Supercritical Solution Method. *Energ. Mater.* **2011**, *19*, 147–151.
9. Shi, X.; Wang, J.; Li, X.; Wang, J. Preparation and characterization of RDX-based composite energetic microspheres. *Chin. J. Energ. Mater.* **2015**, *23*, 428–432.
10. Guo, C.; Jia, X.; Geng, X.; Wang, J.; Hou, C.; Tan, Y. Effect of high temperature water vapor on morphology and thermal decomposition properties of RDX/PMMA. *J. Solid Rocket Technol.* **2018**, *41*, 338–342.
11. Klaumünzer, M.; Pessina, F.; Spitzer, D. Indicating Inconsistency of Desensitizing High Explosives against Impact through Recrystallization at the Nanoscale. *J. Energ. Mater.* **2017**, *35*, 375–384. [CrossRef]
12. Li, X.; Sun, H.; Song, C.; Zhang, X.; Yang, W.; Wang, J. Effect of binder on properties of Cl-20/Fox-7 based PBX. *Chin. J. Explos. Propellant* **2020**, *43*, 51–56.
13. Lal, S.; Staples, R.J.; Jean'ne, M.S. FOX-7 based nitrogen rich green energetic salts: Synthesis, characterization, propulsive and detonation performance. *Chem. Eng. J.* **2023**, *452*, 139600. [CrossRef]
14. Fangjian, S.; Ting, W.; Yinhua, M.; Meiheng, L. Theoretical study on several important decomposition paths of FOX-7 and its derivatives. *Comput. Theor. Chem.* **2022**, *1217*, 113895.
15. Nazin, G.M.; Dubikhin, V.V.; Kazakov, A.I.; Nabatova, A.V.; Krisyuk, B.E.; Volkova, N.N.; Shastin, A.V. Kinetics of the Decomposition of 1,1-Diamino-2,2-Dinitroethylene (FOX-7). Part 4: Comparison of the Decomposition Reactions of FOX-7 and Its Diazacyclic Derivatives. *Russ. J. Phys. Chem. B* **2022**, *16*, 308–315. [CrossRef]
16. Gao, H.F.; Zhang, S.H.; Ren, F.D.; Liu, F.; Gou, R.J.; Ding, X. Theoretical insight into the co-crystal explosive of 2,4,6,8,10,12-hexanitrohexaazaisowurtzitane (CL-20)/1,1-diamino-2,2-dinitroethylene (FOX-7). *Comput. Mater. Sci.* **2015**, *107*, 33–41. [CrossRef]
17. Wei, Y.; Ren, F.; Shi, W.; Zhao, Q. Theoretical insight into the influences of molecular ratios on stabilities and mechanical properties, solvent effect of HMX/FOX-7 cocrystal explosive. *J. Energ. Mater.* **2016**, *34*, 426–439. [CrossRef]
18. Tian, X.; Huang, Y.; Wang, X.; Xu, H.; Li, W.; Zhao, K.; Yang, H.; Li, Y. Influence of Mixture Ratio of FOX-7 and RDX on Slow Cook-off and Shock Sensitivity of Pressed Explosives. *Explos. Mater.* **2019**, *48*, 38–41.
19. Zhou, C.; Chang, P.; Hu, L.; Li, X.; Xiong, C.; Wang, B. Preparation, Characterization and Properties of FOX-7/RDX Composite Explosive. *Chin. J. Explos. Propellant* **2020**, *43*, 669–673+680.
20. Zhou, N.; Zhu, P.; Rong, Y.; Xia, H.; Shen, R.; Ye, Y.; Lv, S. Microfluidic Synthesis of Size-Controlled and Morphologically Homogeneous Lead Trinitroresorcinate Produced by Segmented Flow. *Propellants Explos. Pyrotech.* **2016**, *41*, 899–905. [CrossRef]
21. Shi, J.; Zhao, S.; Jiang, H.; Xu, S.; Zhao, F.; Shen, R.; Ye, Y.; Zhu, P. Multi-size control of homogeneous explosives by coaxial microfluidics. *React. Chem. Eng.* **2021**, *6*, 2354–2363. [CrossRef]
22. Lu, J.; Wang, H.; Pan, J.; Fang, Q. Research progress of microfluidic technology in synthesis of micro/nano materials. *Acta Chim. Sinica* **2021**, *79*, 809–819. [CrossRef]
23. Zhou, J.; Wu, B.; Wang, M.; Liu, S.; Xie, Z.; An, C.; Wang, J. Accurate and efficient droplet microfluidic strategy for controlling the morphology of energetic microspheres. *J. Energ. Mater.* **2021**, 1–18. [CrossRef]
24. Yang, Z.; Zhu, P.; Zhang, Q.; Shi, J.; Wang, K.; Shen, R. Microcrystalline PETN Prepared Using Microfluidic Recrystallization Platform and Its Performance Characterization. *Propellants Explos. Pyrotech.* **2021**, *46*, 1097–1106. [CrossRef]
25. Yu, J.; Xu, S.Y.; Jiang, H.Y.; Zhao, F.Q. Application and Development Trend of Microfluidic Technology in Preparation of Energetic Materials. *Acta Pyrodynamites* **2021**, *6*, 2354–2363.
26. Wu, J.W.; Xia, H.M.; Zhang, Y.Y.; Zhao, S.F.; Zhu, P.; Wang, Z.P. An efficient micromixer combining oscillatory flow and divergent circular chambers. *Microsyst. Technol.* **2018**, *25*, 2741–2750. [CrossRef]
27. Han, R.; Chen, J.; Zhang, F.; Wang, Y.; Zhang, L.; Lu, F.; Wang, H.; Chu, E. Fabrication of microspherical Hexanitrostilbene (HNS) with droplet microfluidic technology. *Powder Technol.* **2021**, *379*, 184–190. [CrossRef]
28. Yazhi, C.; Qian, W.; Hui, R.; Tao, Y. Preparation and Characterization of nAl@PVDF@CL-20 Composite Energetic Particles Assembled via Microfluidic Method. *Chin. J. Energ. Mater.* **2022**, *30*, 1–9.
29. Ruishan, H.; Fang, Z.; Feipeng, L.; Yanlan, W.; Lei, Z.; Jianhua, C.; Rui, Z.; Haifu, W.; Enyi, C. Preparation and Modification Technology of Lead Azide Primary Explosive Based on Microfluidics. *Chin. J. Energ. Mater.* **2022**, *30*, 451–458.
30. Yipeng, F.; Jinyu, S.; Peng, Z.; Ruiqi, S.; Bin, Y.; Anmin, Y.; Enyi, C. Microscale Continuous Flow Preparation and Characterization of Ultra Zr@NC. *Chin. J. Energ. Mater.* **2022**, *30*, 417–423.
31. Jinqiang, Z.; Kai, L.; Yunyan, G.; Rui, Z.; Jiahui, S.; Bidong, W.; Chongwei, A.; Jingyu, W. Preparation of TATB-based PBX Composite Microspheres by Droplet Microfluidic Technology. *Chin. J. Energ. Mater.* **2022**, *30*, 439–445.
32. Li, L.; Ling, H.; Tao, J.; Pei, C.; Duan, X. Microchannel-confined crystallization: Shape-controlled continuous preparation of a high-quality CL-20/HMX cocrystal. *Cryst. Eng. Comm.* **2022**, *24*, 1523–1528. [CrossRef]
33. Li, L.; Yin, T.; Wu, B.; Duan, X.; Pei, C. Preparation of CL-20/HMX Co-crystal by Microchannel Crystallization Based on Solvent/non-solvent Method. *Chin. J. Energ. Mater.* **2021**, *29*, 62–69.